Efficient Monte Carlo Algorithm in Quasi-One-Dimensional Ising Spin Systems

Tota Nakamura

College of Engineering, Shibaura Institute of Technology, Minuma-ku, Saitama 330-8570, Japan

(Received 17 September 2008; published 20 November 2008)

We develop an efficient Monte Carlo algorithm, which accelerates slow Monte Carlo dynamics in quasi-one-dimensional Ising spin systems. The loop algorithm of the quantum Monte Carlo method is applied to the classical spin models with highly anisotropic exchange interactions. Both correlation time and real CPU time are reduced drastically. The algorithm is demonstrated in the layered triangular-lattice antiferromagnetic Ising model. We have obtained the relation between the transition temperature and the exchange interaction parameters, which modifies the result of the chain-mean-field theory.

DOI: 10.1103/PhysRevLett.101.210602 PACS numbers: 05.10.Ln, 05.50.+q, 75.40.Mg

The application of the Monte Carlo (MC) method to condensed-matter physics has been a successful bridge between experimental and theoretical studies [1]. The simulation results are now quantitatively compared with the experimental results. We may estimate various physical parameters, predict unknown properties, and propose new experiments on real materials. However, we encounter a difficulty when we apply the MC method to the frustrated systems. The MC dynamics slows down, and it becomes very hard to reach the equilibrium states. Since frustration has been recognized to play an important role in novel effects of many materials,[2] we somehow have to overcome this difficulty to study new properties, new concepts, and new functions of such materials.

In this Letter we consider the quasi-one-dimensional (Q1D) frustrated spin systems. The magnetic exchange interaction of this system is highly anisotropic. The interaction along the c axis is much stronger than those within the ab plane: $|J_c| \gg |J_{ab}|$. The experimental realizations of this model are the ABX_3-type compounds [3–7]. The lattice structure is the stacked triangular lattice with the antiferromagnetic exchange interactions. There are two reasons for the slow MC dynamics in this system. One is frustration, and the other is the long correlation length along the c axis. The single-spin-flip algorithm cannot change the states of these correlated clusters. Koseki and Matsubara [8–10] proposed the cluster-heat-bath method, which accelerates the MC dynamics in Q1D Ising spin systems. When we update a spin state, the transfer matrix is multiplied along the c axis. This matrix operation takes a long CPU time. The possible size of simulation has been restricted to the system with $|J_c/J_{ab}| = 10$, $36 \times 36 \times 360$ spins, and 2×10^6 MC steps [11]. Considering that the ratio $|J_c/J_{ab}|$ in real compounds is in the order of 100, we need to develop another algorithm that improves the simulation efficiency.

We notice that the similar slow-dynamic situation occurs in the quantum Monte Carlo (QMC) simulation [12]. The d-dimensional quantum system is mapped to the $(d+1)$-dimensional classical system, on which the simulation is performed. The additional dimension is called the Trotter direction, and its length is called the Trotter number. The $(d+1)$-dimensional classical system becomes equivalent to the original d-dimensional quantum system when the Trotter number is infinite. As the Trotter number increases, the correlation length along the Trotter direction increases, and the dynamics of the simulation slows down.

The simulation in the Q1D system is equivalent to the QMC simulation if we regard the Trotter direction as the c axis in the Q1D system. For example, the cluster-heat-bath algorithm in the Q1D system is equivalent to the transfer-matrix MC method [13,14] in QMC simulations. This is the main idea of this paper. We know that the continuous imaginary-time loop flip algorithm of QMC simulation [15–18] is very efficient. Therefore, we apply this QMC algorithm to the Q1D simulation. The correlated cluster along the c axis is flipped by one update trial. We do not suffer from the MC slowing-down due to the long correlation length. The algorithm was successfully applied to the theoretical analysis on the magneto-electric transitions in $RbCoBr_3$ [19]. The numerical results quantitatively agree with the experimental results. The estimates of the interaction parameters and proposals of new experiments were made possible.

We consider the transverse-field Ising model in two dimensions. The Hamiltonian is written as

$$\mathcal{H}_q = -J\sum_{\langle j,k\rangle}\sigma_j^z\sigma_k^z - \Gamma\sum_j \sigma_j^x, \tag{1}$$

where σ^x and σ^z denote the Pauli spin operators, J denotes the exchange interaction parameter, and $\Gamma(>0)$ denotes the transverse field. The indices, j and k, denote the spin location on the two-dimensional real-space plane throughout in this Letter. The brackets $\langle\cdots\rangle$ denote the interacting spin pairs. We apply the Suzuki-Trotter decomposition [12] and map the quantum system $\mathcal{H}_q$ to the effective classical system $\mathcal{H}_c$, which is written as

$$\mathcal{H}_c = \sum_{i=1}^{m}\left(-\frac{J}{m}\sum_{\langle j,k\rangle}\sigma_{i,j}\sigma_{i,k} - \frac{\ln\coth(\frac{\beta\Gamma}{m})}{2\beta}\sum_j \sigma_{i,j}\sigma_{i+1,j}\right). \tag{2}$$

Here, m denotes the Trotter number, β denotes the inverse temperature, and $\sigma_{i,j} = \pm 1$ denotes the Ising spin. The index, i, denotes the location along the Trotter direction throughout in this Letter. The first term of this effective classical system denotes the exchange interaction between spins on the same Trotter slice. The second term is the exchange interaction between spins at the same real-space site with the different (nearest-neighbor) Trotter slice.

The effective classical system can be regarded as the Q1D spin system:

$$\mathcal{H}_{\mathrm{Q1D}} = \sum_{i=1}^{L_c} \left(-J_{ab} \sum_{\langle j,k \rangle} \sigma_{i,j}\sigma_{i,k} - J_c \sum_{j} \sigma_{i,j}\sigma_{i+1,j} \right), \quad (3)$$

if we set

$$J = mJ_{ab}, \quad (4)$$

$$\Gamma = \frac{m}{2\beta} \ln \coth[\beta J_c], \quad (5)$$

$$m = L_c. \quad (6)$$

Here, i denotes the location along the c axis, j and k denote the location on the ab plane, and L_c denotes the linear size along the c axis. The simulation in the Q1D system can be substituted for the QMC simulation with J, Γ, and m defined above. The sign of J_c is positive (ferromagnetic) in this expression. In the case when it is negative (antiferromagnetic), we transform it to the ferromagnetic one by changing the spin notation as $\sigma_{i,j} \to (-1)^i \sigma_{i,j}$.

Let us consider the cluster algorithm of the Q1D system. It is the interpretation of the QMC cluster algorithm [18], where the cluster is only defined along the Trotter direction. We define a cluster using only the J_c part of the Q1D Hamiltonian, and consider the J_{ab} part as the molecular field to the cluster. We may regard this algorithm as the Swendsen-Wang algorithm [20] in one dimension [the J_c part in Eq. (3)] under the molecular field [the J_{ab} part in Eq. (3)]. The ergodicity and the detailed-balance condition are guaranteed.

The updating procedure is as follows. First, we select one location j on the ab plane, and consider the spins along the c axis. We define clusters by connecting the neighboring spins ($\sigma_{i,j}$ and $\sigma_{i+1,j}$) with the following probability p_c:

$$p_c = 1 - \exp[-2\beta J_c] \quad (\sigma_{i,j} = \sigma_{i+1,j}), \quad (7)$$

$$p_c = 0 \quad (\sigma_{i,j} \neq \sigma_{i+1,j}). \quad (8)$$

Let us number the cluster by I. Second, we calculate the molecular field h_I for each updating cluster I as

$$h_I = \sum_{i \in I} \sum_{\langle k \rangle} J_{ab}\sigma_{i,k}, \quad (9)$$

where $i \in I$ denotes that i belongs to the cluster I, and $\langle k \rangle$ denotes that $\sigma_{i,k}$ is interacting with $\sigma_{i,j}$. Finally, we flip the cluster state with the following probability p_I:

$$p_I = \frac{1}{\exp[2\beta\sigma_{i,j}h_I] + 1}. \quad (10)$$

We independently try this flip for each cluster.

The MC correlation time is reduced by this flip but the real CPU time rather increases because we have to do the connecting procedures for all spins along the c axis. We solve this problem by applying the continuous imaginary-time cluster flip algorithm of QMC simulation [16–18]. We neglect the discreteness of the spin location along the c axis. This approximation is possible when both cluster length and L_c are very long.

In the continuous version we focus on the locations of the cluster edges. The probability that the spin pair of $\sigma_{i,j} = \sigma_{i+1,j}$ is not connected is

$$\exp[-2\beta J_c] = \xi_c^{-1}, \quad (11)$$

where ξ_c is regarded as the correlation length along the c axis. The average cluster size coincides with the correlation length ξ_c. If we set $L_c = L_{ab}\xi_c$, the system roughly consists of L_{ab}^3 correlated clusters. It is known that the cluster length obeys the Poisson distribution [17]. We generate the Poisson random numbers with the mean $\exp[2\beta J_c]$ and regard them the cluster length. Then, we place the cluster edges to the c axis from bottom to top. Combining these new-generated cluster edges and the already existing ones, we apply the cluster flip with the probability P_I. The procedure is shown in Fig. 1.

The present continuous c axis version benefits from the memory reduction and the CPU time reduction. We need not memorize all the spin states. Only the locations of the cluster edges and the spin state at the bottom edge are necessary. The total memory use and the real CPU time are

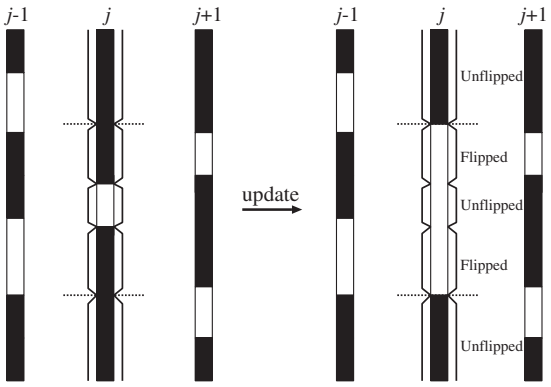

FIG. 1. The updating procedure of the continuous c axis version. Black (white) rectangles depict the up-state (down-state) spin clusters. The new-generated cluster edges are depicted by broken horizontal lines. Brackets depict the clusters to be updated. We update each cluster state independently using the probability p_I.

proportional to L_{ab}^3. Those for the single-spin-flip algorithm are proportional to the total number of spins, $L_{ab}^3 \xi_c$. The efficiency gain, ξ_c, becomes exponentially large at low temperatures.

We apply the continuous c axis cluster flip algorithm to the stacked-triangular lattice antiferromagnetic Ising model. It is a model system for the ABX_3-type compounds [3–7]. The Hamiltonian is written as follows.

$$\mathcal{H} = -2J_c \sum_{i,j} S_{i,j} S_{(i+1),j} - 2J_1 \sum_i \sum_{\langle jk \rangle}^{\text{n.n.}} S_{i,j} S_{i,k} - 2J_2 \sum_i \sum_{\langle jk \rangle}^{\text{n.n.n.}} S_{i,j} S_{i,k}, \quad (12)$$

where $S_{i,j} = \frac{1}{2}\sigma_{i,j}$ is the spin-1/2 Ising spins, and $J_1(J_2)$ denotes the nearest-neighbor (next-nearest-neighbor) exchange interactions within the ab plane. We consider the case where both J_c and J_1 are antiferromagnetic (J_c, $J_1 < 0$), and J_2 is ferromagnetic ($J_2 > 0$).

It is known through theoretical analyses [10,21–23] that successive magnetic phase transitions occur. The low-temperature magnetic structure is the ferrimagnetic state. There exists a partially-disordered (PD) phase between the paramagnetic phase and the ferrimagnetic phase. In the PD phase, one of three sublattices is completely disordered, while the other two sublattices take antiferromagnetic configurations. It is considered that the phase transition between the paramagnetic phase and the PD phase is the second-order transition. We refer to the transition temperature as T_{N1}.

We compare the equilibration and the real CPU time of the present algorithm with the results of the single-spin-flip algorithm. We set $J_c = -97.4$ K, $J_1 = -2.44$ K, $J_2 = 0.142$ K, and perform the simulation at $T = 25$ K. The system is in the ferrimagnetic phase at this temperature. The linear lattice size of the ab plane is set as $L_{ab} = 95$. The correlation length along the c axis is roughly estimated as $\xi_c \sim \exp[\beta|J_c|] = 49$, and the linear size along the c axis is set as $L_c = L_{ab}\xi_c = 4655$. The effective number of spins is more than 42 million. We observe the relaxation functions of the structure factors defined as follows:

$$f_{1/3}^2 = \frac{1}{8}\left\langle \sum_{\eta=\alpha,\beta,\gamma} (m_\eta - m_{\eta+1})^2 \right\rangle, \quad (13)$$

$$f_1^2 = \langle (m_\alpha + m_\beta + m_\gamma)^2 \rangle, \quad (14)$$

where m_α, m_β, and m_γ are three sublattice magnetizations in the triangular lattice. The 1/3-structure factor, $f_{1/3}^2$ takes a finite value when the ferrimagnetic state or the PD state is realized. It detects the phase transition between the PD phase and the paramagnetic phase. The phase transition between the PD phase and the ferrimagnetic phase is detected by the structure factor, f_1.

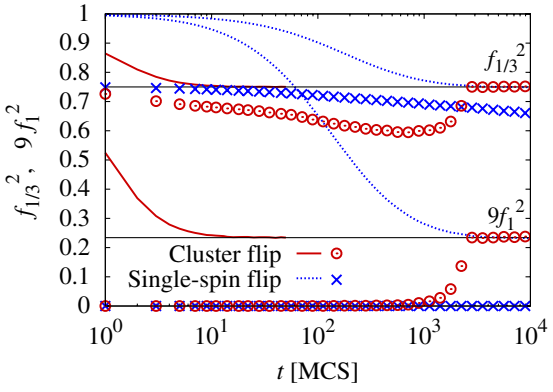

FIG. 2 (color online). The relaxation function of the structure factors, $f_{1/3}^2$ and $9f_1^2$, when the simulations start from the ferrimagnetic state (lines) and the PD state (symbols).

Figure 2 shows the relaxation functions of both structure factors. We start the simulations from the perfect ferrimagnetic state ($f_{1/3}^2 = 1$ and $f_1^2 = 1/9$, plotted with lines) and the perfect PD state ($f_{1/3}^2 = 3/4$ and $f_1^2 = 0$, plotted with symbols). The data of two algorithms converge to the same value. It guarantees the equilibration of the simulation. The cluster algorithm realizes the equilibrium state roughly 300 times earlier than the single-spin-flip algorithm. The convergence is slow when the initial state is the PD state. In this case, the single-spin-flip algorithm fails to reach the equilibrium state within the present MC steps. Table I compares the real CPU time. The present cluster algorithm achieves simulation 15 times faster. This difference comes from the ratio $L_c/L_{ab} = \xi_c$.

We focus on the transition temperature between the paramagnetic phase and the PD phase, T_{N1}. The chain-mean-field theory [21] gives the relation among T_{N1}, J_1, and J_c, which is written as

$$1 = \frac{\exp[\frac{|J_c|}{k_B T_{\text{N1}}}]}{2k_B T_{\text{N1}}}(-3J_1 + 6J_2). \quad (15)$$

Using the present cluster algorithm we estimate T_{N1} for various choices of J_1/J_c ranging from 0.001 to 0.5 and J_2/J_c ranging from -0.05 to -0.0015. The behavior of T_{N1} with respect to J_c, J_1, and J_2 is obtained. Here, the nonequilibrium relaxation method [24] is applied. We obtain the transition temperature by the behavior of the relaxation functions of the structure factor, $f_{1/3}^2$. It con-

TABLE I. The real CPU time for each Monte Carlo step is compared. The simulations were performed on the Core 2 Duo E6600 processor at 2.4 GHz using the Intel compiler.

MC steps [MCS]	Cluster flip [s]	Single-spin flip [s]
100	39	568
200	77	1155
500	195	2910
10000	3919	58560

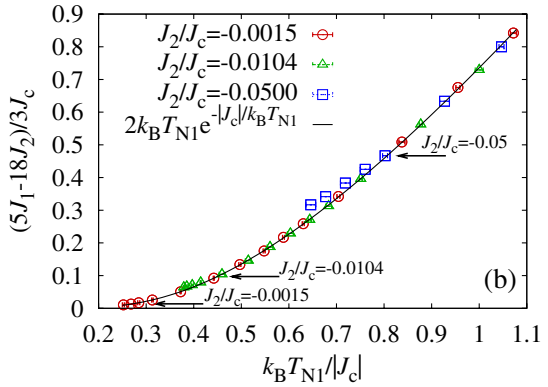

FIG. 3 (color online). Relation between the exchange interaction parameters and the transition temperature T_{N1} obtained by the Monte Carlo simulation. Arrows depict the point where $|J_2| = |J_1|/2$ for each choice of J_2/J_c. The numerical results fall onto the single function as long as $|J_2| < |J_1|/2$.

verges to the finite value when the temperature is below T_{N1} and decays exponentially when the temperature is above T_{N1}. The algebraic decay is exhibited at T_{N1}.

We find that most of our numerical results are well-fitted by the following expression.

$$1 = \frac{\exp[\frac{|J_c|}{k_B T_{N1}}]}{2k_B T_{N1}}\left(-\frac{5}{3}J_1 + 6J_2\right). \quad (16)$$

Only the coefficient of J_1 differs from the chain-mean-field result. The change of the coefficient can be regarded as the reduction of the effective coordination number [25]. The fitting is plotted in Fig. 3. The arrows in the figure depict the data when $|J_2| = |J_1|/2$ for each choice of J_2. The data deviate from the relation, Eq. (16), when $|J_2| > |J_1|/2$. Since the chain-mean-field relation, Eq. (15), has been used to estimate the interaction parameter from the experimental results, the present relation, Eq. (16), improves the estimate.

We have introduced the cluster flip algorithm suitable for the quasi-one-dimensional frustrated Ising spin systems. The numerical efficiency is improved as we lower the temperature and/or as we increase the anisotropy ratio, $|J_c/J_{ab}|$. Other algorithms mostly fail in this situation. The realistic simulations (or emulations) for real compounds are made possible. The quantitative MC analyses to the experimental results may help developments in material science. Simulations under the magnetic field are possible. We may include the field term into the molecular field term, h_I.

The use of random number generator RNDTIK programmed by Professor N. Ito and Professor Y. Kanada is gratefully acknowledged.

[1] *The Monte Carlo Method in Condensed Matter Physics*, edited by K. Binder (Springer-Verlag, Berlin, 1995).
[2] For example, articles in *Proceedings of the International Conference on Highly Frustrated Magnetism, Osaka, Japan, 15-19 August 2006* , [J. Phys. Condens. Matter 19, (2007)].
[3] W. B. Yelon, D. E. Cox, and M. Eibschütz, Phys. Rev. B **12**, 5007 (1975).
[4] M. Mekata and K. Adachi, J. Phys. Soc. Jpn. **44**, 806 (1978).
[5] D. Visser, G. C. Verschoor, and D. J. W. Ijdo, Acta Crystallogr. Sect. B **36**, 28 (1980).
[6] Y. Nishiwaki, H. Imamura, T. Mitsui, H. Tanaka, and K. Iio, J. Phys. Soc. Jpn. **75**, 094702 (2006).
[7] Y. Nishiwaki, T. Nakamura, A. Oosawa, K. Kakurai, N. Todoroki, N. Igawa, Y. Ishii, and T. Kato, J. Phys. Soc. Jpn. **77**, 104703 (2008).
[8] O. Koseki and F. Matsubara, J. Phys. Soc. Jpn. **66**, 322 (1997).
[9] F. Matsubara, A. Sato, O. Koseki, and T. Shirakura, Phys. Rev. Lett. **78**, 3237 (1997).
[10] O. Koseki and F. Matsubara, J. Phys. Soc. Jpn. **69**, 1202 (2000).
[11] E. Meloche and M. L. Plumer, Phys. Rev. B **76**, 174430 (2007).
[12] *Quantum Monte Carlo Methods in Condensed Matter Physics*, edited by M. Suzuki (World Scientific, Singapore, 1994).
[13] S. Miyashita, J. Phys. Soc. Jpn. **63**, 2449 (1994).
[14] T. Nakamura and S. Miyashita, Phys. Rev. B **52**, 9174 (1995).
[15] H. G. Evertz, G. Lana, and M. Marcu, Phys. Rev. Lett. **70**, 875 (1993).
[16] U.-J. Wiese and H.-P. Ying, Z. Phys. B **93**, 147 (1994).
[17] H. G. Evertz, Adv. Phys. **52**, 1 (2003).
[18] T. Nakamura and Y. Ito, J. Phys. Soc. Jpn. **72**, 2405 (2003).
[19] T. Nakamura and Y. Nishiwaki, Phys. Rev. B **78**, 104422 (2008).
[20] R. H. Swendsen and J.-S. Wang, Phys. Rev. Lett. **58**, 86 (1987).
[21] H. Shiba, Prog. Theor. Phys. **64**, 466 (1980).
[22] F. Matsubara and S. Inawashiro, J. Phys. Soc. Jpn. **53**, 4373 (1984).
[23] N. Todoroki and S. Miyashita, J. Phys. Soc. Jpn. **73**, 412 (2004).
[24] Y. Ozeki and N. Ito, J. Phys. A **40**, R149 (2007), and references therein.
[25] S. Todo, Phys. Rev. B **74**, 104415 (2006).